

Direct Speed Control of PMSM Drive Using SDRE and Convex Constrained Optimization

Václav Šmídl, *Member, IEEE*, Štěpán Janouš, Lukáš Adam, Zdeněk Peroutka, *Member, IEEE*

Abstract—The challenge for control of PMSM drives is to achieve high dynamics, accurate steady state performance and respect all constraints on input voltage and stator currents. Many partial results on each of these aspects are available. Recently, it has been shown that existing techniques can be combined with ideas from predictive control to achieve satisfaction of state constraints such as maximum current amplitude. In this paper, we propose to complement the direct speed control based state-dependent Riccati equation (SDRE) approach by explicit constraints on the current amplitude and the field weakening curve. Since cost-to-go function for SDRE is available, the problem is formulated as quadratic programming with quadratic constraint. The resulting controller achieves excellent steady state solution due to SDRE and satisfies constraints on the maximum current amplitude and field weakening operation. Experimental tests of the proposed cascade-free speed control are performed on a laboratory prototype of a 10.7 kW PMSM drive. The proposed optimization routine can be used to enforce state constraints in other unconstrained control methods.

I. INTRODUCTION

Satisfaction of operational constraints on input voltage and stator currents is one of the key requirements on drive control. These constraints can be easily handled in the conventional cascade control. Decomposition of the control problem into the speed, torque and current loops is an intuitive way how to understand the problem and thus, it is favored by many practitioners. Modern optimal control theory is however based on state space models [1] avoiding cascades and loops. Application of the theoretical results from optimal control to drive control have been presented long time ago [2], however, they never reached popularity. One of potential reasons is that the optimal control solution lacked the ability to naturally impose hard constraints in a simple and understandable way. Therefore, even very recent optimal control approaches [3], [4], [5] do not consider the constraints. Constraints on the stator current amplitude can be handled e.g. by an antiwindup approach [5], [6]. However, antiwindup does not address the field weakening problem.

Manuscript received Month 05, 2016; revised Month 03, 2017; accepted Month 6, 2017. This research has been supported by the Ministry of Education, Youth and Sports of the Czech Republic under the RICE – New Technologies and Concepts for Smart Industrial Systems, project No. LO1607. V.Šmídl, Š. Janouš and Z. Peroutka are with the Regional Innovation Centre for Electrical Engineering University of West Bohemia, Pilsen, Czech Republic, email: smidl@utia.cas.cz, peroutka@ieee.org. L. Adam is with the Institute of Information Theory and Automation, Prague, Czech Republic.

A more complex approach that is able to handle more complex constraints is the predictive control. The interest in optimal control approaches has been increased due to success of the model predictive control, especially in combination with a finite set of control actions (FCS-MPC) [7]. Predictive control allows to consider hard constraints, however, the constraints on the limited supply voltage require special treatment. In [8], [9] it was proposed to use one step optimization with carefully designed constraints and attraction regions. In [10], the attraction regions were replaced by an approximation of the cost-to-go function and the result used in the FCS-MPC approach. Nevertheless, the FCS-MPC also has its weak points, such as variable switching frequency resulting in spread frequency spectrum of converter currents, and operation at lower switching frequencies resulting in higher current ripple. Extension of predictive torque control to direct (cascade-free) speed control of PMSM has been presented in [11]. The finite control set was used since the same optimization in continuous control set (CCS) would be too expensive. Continuous control set optimization has been used in [12], [13] where the problem was simplified using cascade structure of PI controller providing torque reference and predictive torque controller. We aim to extend this work to direct speed control without the need for cascades.

To achieve this aim, we follow a simplified solution which combines unconstrained solution with constraints optimization that is applied after calculation of the unconstrained solution. This idea has been proved theoretically in [14] and already used in PMSM control e.g. in [6] in simpler settings. We intend to impose constraints on the current amplitude, as well as on the field weakening operation. The problem is then decomposed into two parts: (i) derivation of an unconstrained solution, and (ii) how to solve the constrained optimization problem. Since we require cost-to-go function, we can use existing methods based on SDRE approach [3], [4] or non-linear predictive control [5]. We have chosen the former for its simplicity. Optimization of the operating constraints for torque control is often concerned with projection to MTPA curve which can be achieved approximately using intersections of linear curves [15], or exactly solving roots of fourth order polynomial [12]. Perhaps, the most complex optimization task has been presented in [16] which is computationally costly and was implemented in FPGA.

In this paper, we propose to use SDRE as an optimal direct speed controller for unconstrained problem. We impose the same operational constraints as in [12], i.e. the current amplitude limit and the field weakening limit. We show that since SDRE optimizes also the Joule losses, its current

trajectory closely follows MTPA and it is not necessary to impose it as an additional constraint. In effect, the proposed controller follows exactly the SDRE control law when the constraints are not active. The mathematical model is used to predict the future current to check if the constraints are not violated. If the potential constraint violation is detected, the predicted current is projected to the feasible region and the input voltage vector is modified to yield the constrained current.

II. PREDICTIVE SPEED CONTROL OF PMSM DRIVE

In this section we combine several techniques of cascade-free speed control of PMSM drives. After review of known results from [8], [9], [10], [4], we formulate the main optimization problem. Solution of the optimization problem is proposed in the next section.

A. Model of the drive

Consider the conventional state space equations of PMSM drive

$$\frac{di_d}{dt} = -\frac{R_s}{L_d}i_d + \frac{L_q}{L_d}i_q\omega + \frac{1}{L_d}u_d, \quad (1)$$

$$\frac{di_q}{dt} = -\frac{R_s}{L_q}i_q - \frac{\Psi_{PM}}{L_q}\omega - \frac{L_d}{L_q}i_d\omega + \frac{1}{L_q}u_q, \quad (2)$$

$$\frac{d\omega}{dt} = \frac{1}{J} \left[\frac{3}{2}p_p^2 (\Psi_{PM}i_q + (L_d - L_q)i_d i_q) - p_p T_L \right], \quad (3)$$

$$\frac{d\vartheta}{dt} = \omega, \quad (4)$$

$$\frac{dT_L}{dt} = \delta, \quad (5)$$

The state vector $x = [i_d, i_q, \omega, \vartheta, T_L]$ is composed of components of the stator current vector (i_d, i_q) of the drive in rotating (d - q) reference frame linked to a rotor flux, the electrical rotor speed ω , the electrical rotor position ϑ , load torque T_L . Input of the state space model are components of the stator voltage vector u_d, u_q . The system parameters are: the components of the stator inductance L_d, L_q , the stator resistance R_s , the flux linkage excited by permanent magnets on the rotor Ψ_{PM} , and the number of pole pairs p_p . We assume that the load torque is changing linearly in time, with derivative δ , which is assumed to be known.

In general, the model is non-linear due to products of state variables. Many techniques for local linearization can be used. In this paper, we focus on a method based on two simplifications: (i) we consider the rotor speed ω to be constant during the sampling period; and (ii) the product $i_d i_q$ is approximated by first order Taylor expansion. The first simplification allows us to approximate the products $i_d \omega$ and $i_q \omega$ by linear terms $i_d \omega^{op}$ and $i_q \omega^{op}$, where ω^{op} is the operational point of the rotor speed. In the resulting algorithm it will be replaced by instantaneous speed. First order Taylor approximation of the non-linear term in (3) is

$$i_d i_q \approx -i_d^{op} i_q^{op} + i_d^{op} i_q + i_d i_q^{op}, \quad (6)$$

where i_d^{op} and i_q^{op} are components of stator current vector at the operational point. They will be also replaced by instantaneous currents.

Under these simplifications, model (1)–(5) can be rewritten in standard linear form $dx/dt = A_c(x^{op})x + B_c u$ where $x^{op} = [i_d^{op}, i_q^{op}, \omega^{op}, 0, 0]$. To accommodate for the constant term $-i_d^{op} i_q^{op}$ from (6), we assume that the state vector is extended to contain additional constant, i.e. $x = [i_d, i_q, \omega, \vartheta, T_L, 1]$. This is an auxiliary step allowing the use of standard software, that has no impact on physical interpretation of the model.

Conversion of the model into discrete time form with sampling time Δt is achieved using the conventional discretization formula

$$A(x^{op}) = e^{A_c(x^{op})\Delta t},$$

$$B(x^{op}) = \int_0^{\Delta t} e^{A_c(x^{op})(\Delta t - \tau)} B_c d\tau.$$

The resulting state-dependent linear system is then

$$x_{t+1} = A(x^{op})x_t + B(x^{op})u_t. \quad (7)$$

Matrices $A(x^{op})$ and $B(x^{op})$ are computed in Matlab using routine `expm()`.

B. Predictive speed control

Predictive control in discrete time is defined as an optimization task on receding horizon of length h , minimizing a chosen cost function. In general formalism, we seek solution of task

$$u_{t:t+h}^{opt} = \arg \min_{u_{t:t+h} \in U} \sum_{\tau=t+1}^{t+h} g(x_\tau, u_\tau, x_\tau^*, u_\tau^*), \quad (8)$$

subject to: $u_\tau \in U, x_\tau \in \mathcal{X}, \forall \tau = t+1, \dots, t+h$,

where g is the chosen cost function, U is the set of admissible inputs and \mathcal{X} is the set of allowed system states. Index τ is a running time on prediction horizon from the current time t to $t+h$ where h is the potentially infinite horizon. Star in the upper index denotes requested value of the symbol, e.g. x^* is requested value of the state.

In the context of speed control of PMSM drives, the cost function is designed to reach two objectives: (i) speed tracking, (ii) drive efficiency. These two requirements can be formalized as minimization of the tracking error

$$g_T = (\omega_t - \omega_t^*)^2, \quad (9)$$

and minimization of the current amplitude

$$g_I = (i_{d,t}^2 + i_{q,t}^2). \quad (10)$$

Since these two requirements are contradictory, we need to define a compromise between them, typically in the form of weighted sum

$$g = g_T + \lambda g_I, \quad (11)$$

where $\lambda > 0$ is the chosen factor of the trade-off. For low values of λ speed tracking is preferred over drive efficiency.

The set of admissible control actions is given by maximum amplitude of the input stator voltage $U_{max} = \frac{U_{dc}}{\sqrt{3}}$ (where U_{dc} is converter dc-link voltage) and admissible stator current amplitude, I_{max}

$$\mathcal{X} = \{i : |i| \leq I_{max}\}, \quad U = \{u_t : |u_t| \leq U_{max}\}. \quad (12)$$

We assume that the current limit I_{\max} is a fixed value, but U_{\max} is changing with U_{dc} which is measured.

Solution of the full optimization problem is difficult even numerical solutions on very long horizons failed to find an acceptable solution [17]. In the following sections, we review existing partial solutions proposed in the literature.

C. Unconstrained speed control

Without the constraints on the current and voltage limit (12), the control problem has to deal with non-linear terms in model (1)–(5). One possibility is to linearize the model at the operational point x^{op} and design linear quadratic controller at this point [4]. We follow this idea using simpler tools.

1) *SDRE controller at operational point*: At operational state x^{op} , the model of PMSM is a linear system (7) with quadratic cost functions (9) and (10). In matrix notation, the cost function can be written as

$$g(x_t, u_t, x_t^*, u_t^*) = (x_t - x_t^*)^T Q (x_t - x_t^*) + (u_t - u_{t-1})^T R (u_t - u_{t-1}). \quad (13)$$

where the state reference $x_t^* = [i_{d,t}^*, i_{q,t}^*, \omega_t^*, \vartheta_t^*, T_{L,t}^*, 1]$ is assumed to be constant. In (13) we have used additional cost penalizing difference of the input variable. This penalization is used to suppress steady state error of the resulting controller.

Synthesis of controllers for linear system (7) with quadratic cost (13) can be achieved by pole placement or Riccati equation. We will follow the latter approach. Due to the used penalization of the input difference, we need to augment the state vector to obtain the standard form. The augmented vector is $\tilde{x}_t = [x_t^T, x_t^{*T}, u_{t-1}^T]^T$ with state dynamics

$$\begin{bmatrix} x_{t+1} \\ x_{t+1}^* \\ u_t \end{bmatrix} = \underbrace{\begin{bmatrix} A(x^{\text{op}}) & 0 & 0 \\ 0 & I & 0 \\ 0 & 0 & 0 \end{bmatrix}}_A \begin{bmatrix} x_t \\ x_t^* \\ u_{t-1} \end{bmatrix} + \underbrace{\begin{bmatrix} B(x^{\text{op}}) \\ 0 \\ I \end{bmatrix}}_B u_t,$$

and quadratic cost function

$$g(x_t, u_t, x_t^*, u_t^*) = \tilde{x}_t^T \tilde{Q} \tilde{x}_t + u_t^T R u_t + 2\tilde{x}_t^T N u_t, \quad \tilde{Q} = \begin{bmatrix} Q & -Q & 0 \\ -Q & Q & 0 \\ 0 & 0 & R \end{bmatrix}, \quad N = [0, 0, -R].$$

The optimal control is found by solving the state dependent discrete time Riccati equation,

$$\tilde{A}^T S \tilde{A} - S - (\tilde{A}^T S \tilde{B} + N)(\tilde{B}^T S \tilde{B} + R)^{-1}(\tilde{B}^T S \tilde{A} + N^T) + \tilde{Q} = 0, \quad (14)$$

for matrix variable S . Many tools such as Matlab `dlqr` are available for this task.

Since \tilde{A} is state dependent, the resulting S is also state dependent. The matrix $S(x^{\text{op}})$ defines the cost-to-go function of dynamic programming on infinite horizon [1]

$$V(\tilde{x}_{t+1}) = \tilde{x}_{t+1}^T S(x^{\text{op}}) \tilde{x}_{t+1}, \quad (15)$$

The SDRE controller is thus the optimizer of the following optimization problem

$$u_t^{\text{unc}} = \arg \min_{u_t(x_t)} \{ (u_t + L\tilde{x}_t)^T Y (u_t + L\tilde{x}_t) \} \quad (16)$$

$$L = Y^{-1}(\tilde{B}^T S \tilde{A} + N^T), \quad Y = (\tilde{B}^T S \tilde{B} + R).$$

Which is well known to be

$$u_t^{\text{unc}} = -L(x^{\text{op}})\tilde{x}_t. \quad (17)$$

where $L(x^{\text{op}})$ was used to emphasize the fact that the gain matrix is state dependent.

Remark 1. Quadratic form of the cost-to-go function is very common to many approximate control design method, including non-linear forms [5]. The constrained optimization method designed in this paper can thus be applied to any control scheme that fits into formulation (16).

2) *Implementation using gain scheduling*: In order to avoid online evaluation of the gain $L(x^{\text{op}})$ or its approximation by Taylor expansion, we seek explicit parametric form of the gain using the interpolation method. This is typically more accurate approach [18]. Specifically, we solve the LQR problem for a range of operational states $X^{\text{op}} = [x^{\text{op}(1)}, x^{\text{op}(2)}, \dots, x^{\text{op}(N)}]$ and then solve the regression problem

$$L_{i,j}(x^{\text{op}(n)}) = \alpha_{i,j} \psi(x_k^{(n)}), \quad \forall k = 1, \dots, N \quad (18)$$

with $\psi(x) = [i_d, i_q, \omega, i_d i_q, i_d \omega, i_q \omega, i_d^2, i_q^2, \omega^2, i_d^2 \omega, i_q^2 \omega]$ using the least squares fit. Technically, it is possible to consider higher order polynomials, but the computational cost of its evaluation is growing without improving the quality.

All of the above operations are implemented in Matlab. The result of this computation is a set of coefficients $\alpha_{i,j}$ that are transferred to the DSP. On-line computation in DSP is then reduced to summation and multiplication of these constants and state variables using (18) and (17).

3) *State reconstructor*: The SDRE controller assumes a perfectly known state vector x_t . However, it is usually not available, and its reconstruction has to be designed. Many methods for design of state reconstructors can be applied here. Due to duality of linear quadratic control and Kalman filtering [19], we use the standard Kalman filter for state reconstruction from observations $y_t = [i_{d,t}^{\text{meas}}, i_{q,t}^{\text{meas}}, \vartheta_t^{\text{meas}}]$. The vector of observations is composed of the observed rotor position $\vartheta_t^{\text{meas}}$ which is also used to transform the measured currents to the d - q reference frame. For efficient implementation, we do not compute the Kalman gain online. Once again, we use the gain scheduling idea, precompute the Kalman gain on a grid of state variables and approximate the state-dependent gain $K(x^{\text{op}})$. The computationally efficient state reconstruction is then

$$\hat{x}_t = A(x^{\text{op}})x_{t-1} + B(x^{\text{op}})u_{t-1} + K(x^{\text{op}})(y_t - Cx_{t-1}). \quad (19)$$

Since covariance matrices of the measurement error and especially the model error are not known, they are tuned manually.

D. Speed control with state constraints

An elegant solution of the complex optimization problem (8) has been presented in [11]. The solution is computed on a short prediction horizon h which would yield poor performance with the original cost. Therefore, the cost function (8) is augmented by additional penalizations for deviations of the state from the steady state solutions. Two notable solutions are used. First, the maximum torque per ampere (MTPA) rule [8]

$$\text{MTPA} : \quad i_d + \frac{L_d - L_q}{\Psi_{PM}} (i_d^2 - i_q^2) = 0. \quad (20)$$

which is optimal steady state solution for the current constraint. The second solution is a steady state solution on voltage constraint, the field-weakening curve:

$$\text{FW} : \left(\frac{L_q}{L_d} i_q \right)^2 + \left(i_d + \frac{\Psi_{PM}}{L_d} \right)^2 = \left(\frac{\zeta U_{\max}}{|\omega| L_d} \right)^2, \quad (21)$$

where $\zeta \in [0, 1]$ is a chosen safety factor [8]. This safety factor is used to model the fact that output voltage of a converter is actually lower than that of the dc-link due to voltage drops, dead times and other effects. Since U_{\max} has the role of steady state value, the approximation of the converter by a manually tuned factor ζ is simple and sufficient. Another additive term in the cost function of [11] is penalization current trajectory outside the FW curve. Note that the FW curve is changing with the speed but also with the U_{\max} as it is a function of the actual dc-link voltage. We consider U_{\max} to be an operating point of the controller and change its value in each sampling period using the latest measurement of the dc-link voltage. The solution of this optimization was presented for finite-control set since equivalent optimization in continuous control set would be too expensive.

The closest solution of this problem in continuous control set was presented in [12], [13] using a cascade structure. The speed error is propagated through a PI controller to generate the torque reference. The torque reference is optimized to satisfy the constraints on the maximum amplitude of the current and the field weakening curve. The efficiency of the drive (second term of the cost function (10)) is achieved by using intersection of the torque isoline with the MTPA curve (20). The intersection is then used as a reference for subsequent current controller. If the intersection of the MTPA and the torque isoline is outside of the feasible region, the current setpoint is computed using intersections with the field weakening curve (21) or other important points, see [12] for full details.

In this paper, we aim to solve a direct speed control without the cascade approximation to allow for direct interaction between the torque and current dynamics. Since SDRE optimizes the drive efficiency via (10), we conjecture that it is sufficient only to impose hard constraints on the current limit and the field weakening curve. This idea has been advocated in [6] for the current limit.

E. Optimization problem formulation

The main proposition of this paper is approximation of the optimal control problem (8) by one-step-ahead approximation of the SDRE cost-to-go function (16) with additional constraints on the current limit I_{max} and the FW limit. The final optimization problem is then:

$$u_t^{\text{opt}} = \arg \min_{u_t} \{ (u_t + L\tilde{x}_t)^T Y (u_t + L\tilde{x}_t) \} \quad (22)$$

subject to:

$$c_1 : \quad i_{d,t+1}^2 + i_{q,t+1}^2 \leq I_{\max}^2, \quad (23)$$

$$c_2 : \quad (i_d^\Psi + i_{d,t+1})^2 + \xi i_{q,t+1}^2 \leq I_{FW}^2, \quad (24)$$

$$c_3 : \quad |u_t| \leq U_{\max} \quad (25)$$

The first constraint is the current constraint on one-step ahead prediction (12). The second constraint is the field weakening (21) with substitutions $i_d^\Psi = \frac{\Psi_{PM}}{L_d}$, $\xi = \frac{L_q^2}{L_d^2}$, and $I_{FW} = \zeta \frac{U_{\max}}{|\omega| L_d}$. The third is the voltage limit (12). In principle, it is possible to use any other method providing cost-to-go, e.g. [10], approximated at the operating point by a quadratic approximation.

III. CONVEX CONSTRAINED OPTIMIZATION

The main contribution of this paper is an efficient and simple algorithm for constrained optimization, solving (22)–(24). For clarity of explanation, we reformulate the problem to the current space, where most of the constraints are defined. Formulation in the voltage space is also possible, however, it would not be as intuitive.

A. Task reformulation

We note that the stator current vector i_{t+1} is modeled by a first order model

$$i_{t+1} = A_i(x_t) i_t + B_i u_t, \quad (26)$$

where $A_i(x_t)$ and B_i are blocks of the matrices $A(x^{\text{op}})$ and $B(x^{\text{op}})$ from (7) corresponding to the current equations and u_t is stator voltage vector. Since matrix B_i is invertible,

$$u_t = B_i^{-1} (i_{t+1} - A_i(x_t) i_t),$$

which can be substituted to (22) yielding

$$i_{t+1}^{\text{opt}} = \arg \min_{i_{t+1}} \{ (i_{t+1} - i_{t+1}^{\text{unc}})^T \Phi (i_{t+1} - i_{t+1}^{\text{unc}}) \} \\ \text{subject to: } c_1(i_{t+1}), c_2(i_{t+1}), c_3(i_{t+1}) \quad (27)$$

where $\Phi = B_i^{-T} Y B_i^{-1}$ with Choleski decomposition $\Phi^{\frac{1}{2}}$, $\Phi = (\Phi^{\frac{1}{2}})^T \Phi^{\frac{1}{2}}$, and $i_{t+1}^{\text{unc}} = A_i(x_t) i_t + B_i u_t^{\text{unc}}$ is the projection of the unconstrained control input to the current space.

Further simplification can be achieved by one-to-one transformation $\tilde{i}_{t+1} = \Phi^{\frac{1}{2}} i_{t+1}$ under which the optimization problem becomes

$$\tilde{i}_{t+1}^{\text{opt}} = \arg \min_{\tilde{i}_{t+1}} \{ (\tilde{i}_{t+1} - \tilde{i}_{t+1}^{\text{unc}})^T (\tilde{i}_{t+1} - \tilde{i}_{t+1}^{\text{unc}}) \} \\ \text{subject to: } |\Phi^{-\frac{1}{2}} \tilde{i}_{t+1}| < I_{\max}, \quad (28) \\ |\Xi \Phi^{-\frac{1}{2}} (\tilde{i}_{t+1} - \tilde{i}_{t+1}^{\Psi})| < I_{FW},$$

where $\tilde{i}_{t+1}^{\Psi} = \Phi^{\frac{1}{2}} \begin{bmatrix} i_d^\Psi \\ 0 \end{bmatrix}$, $\Xi = \begin{bmatrix} 1 & 0 \\ 0 & \sqrt{\xi} \end{bmatrix}$, and $\tilde{i}_{t+1} = \Phi^{\frac{1}{2}} A_i(x_t) i_t$. The optimization problem (28) will be solved for $\tilde{i}_{t+1}^{\text{opt}}$ and the optimal stator voltage vector found as

$$u_t^{\text{opt}} = B_i^{-1} (\Phi^{-\frac{1}{2}} \tilde{i}_{t+1}^{\text{opt}} - A_i(x_t) i_t), \quad (29)$$

under constraint $|B_i^{-1} \Phi^{-\frac{1}{2}} (\tilde{i}_{t+1} - \tilde{i}_{t+1}^{\text{opt}})| \leq U_{max}$ which is equivalent to CCS controller of [12].

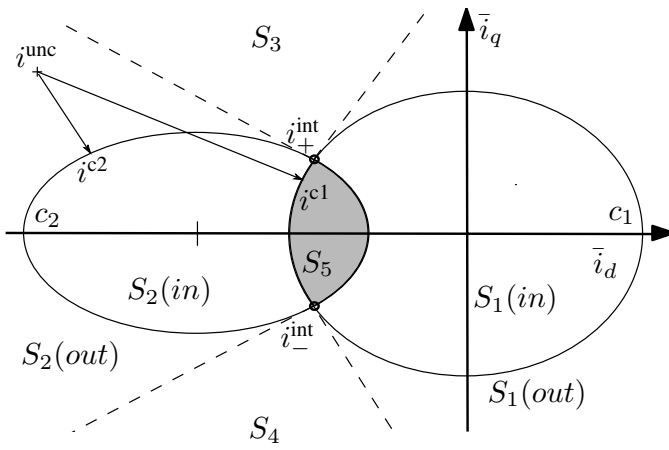


Figure 1. Decomposition of the space for optimal solutions, dashed lines denote normals to the ellipses at their intersection. Feasible set S_5 is denoted by gray area. Illustration of projection of unconstrained solution i^{unc} to ellipse c_1 is denoted by i^{c1} and projection to ellipse c_2 by i^{c2} . Intersection of ellipses is denoted by i_{+}^{int} and i_{-}^{int} .

B. Simplified solution

We derive a simplified optimization algorithm based on the assumptions that the matrix Φ is diagonal and thus axis of all constraining ellipses are aligned with the d - q coordinate system¹. Without loss of generality, we assume that the SDRE solution has form $\Phi = \text{diag}([1, \phi^2])$. Moreover, we assume that the optimization problem is dominated by constraints c_1 and c_2 , which define the optimal predicted current. The third constraints limits only the speed with which it can be reached. Therefore, we first focus on solution of the constraints c_1 and c_2 simplified using the above assumption to

$$c_1 : \quad \bar{i}_d^2 + \bar{i}_q^2 \phi^{-2} \leq I_{max}^2, \quad (30)$$

$$c_2 : \quad (\bar{i}_d + i_d^\psi)^2 + \bar{i}_q^2 \phi^{-2} \xi \leq I_{FW}^2, \quad (31)$$

i.e. two ellipsis centers $[0, 0]$, $[-i_d^\psi, 0]$ and radii $[I_{max}, I_{max}\phi]$, $[I_{FW}, I_{FW}\phi\xi^{-0.5}]$, respectively. Since all variables are in time $t+1$, we omit its explicit mentioning in the notation for clarity.

The optimization problem (28) is essentially minimization of Euclidean distance to the unconstrained solution i^{unc} , hence the optimum solution is obtained by projection onto the feasible set, as illustrated in Figure 1. This general task of convex optimization can be solved by geometric intuition:

- 1) In lower speed region, only constraints c_1 can be violated. The optimal solution is then a projection of i^{unc} to ellipse c_1 (Appendix A), which will be denoted i^{c1} . If the constraint is not violated $i^{c1} = i^{unc}$.
- 2) If only constraint c_2 is violated, the optimal solution is projection of i^{unc} to c_2 which will be denoted i^{c2} .
- 3) Loaded operation at high speed requires to operate the machine at the intersection of ellipses c_1 and c_2 . Efficient algorithm for computing the intersection points i^{int} is given in Appendix B.

The key question is which of the three cases above is optimal at the current state. Decisions based on comparing speed

¹Extension to general case is possible but it would involve additional rotations that are not needed in many applications.

Algorithm 1 Selection of optimal current projection

Input: prediction of unconstrained optimal current (i^{unc})

- 1: $i^{c1} := \text{project}(i^{unc}, c_1)$
- 2: $i^{c2} := \text{project}(i^{unc}, c_2)$
- 3: **if** $(i_d^{c1} + i_d^\psi)^2 + (i_q^{c1})^2 \phi^{-2} \xi \leq I_{FW}^2$ **then** $\triangleright S_2$ or S_5
- 4: $i^{opt} := i^{c1}$
- 5: **else** $\triangleright S_1, S_3, S_4$
- 6: **if** $(i_d^{c2})^2 + (i_q^{c2})^2 \phi^{-2} \leq I_{max}$ **then** $\triangleright S_1$ or S_5
- 7: $i^{opt} := i^{c2}$
- 8: **else** $\triangleright S_3, S_4$
- 9: **if** $I_{FW} + I_{max} > i_d^\psi$ **then** \triangleright Intersection exists
- 10: $i_{+}^{int} := \text{intersect}(c_1, c_2)$
- 11: $i_{-}^{int} := i_{+}^{int}$
- 12: $i_q^{opt} := \text{sgn}(i_q^{unc}) i_q^{int}$
- 13: **else** \triangleright Secure c_1 , ignore c_2
- 14: $i^{opt} := [-I_{max}, 0]$
- 15: **end if**
- 16: **end if**
- 17: **end if**

Output: constrained optimal predicted current (i^{opt})

with reference has been proposed [12], however, they are not optimal in transients. Therefore, we propose a new solution based on convex optimization results.

Note from Figure 1, that the optimal projection depends on the position of the vector i^{unc} in the current plane. If the unconstrained current vector i^{unc} belongs to S_2 , the optimal solution is projection i^{c1} . In such a case, projection i^{c2} will lie outside of constraint c_1 , i.e. $i^{c2} \notin c_1$. This combination of $i^{c1} \in c_2$ and $i^{c2} \notin c_1$ is unique for S_2 . The full set of equivalences is then

$$\begin{aligned}
 i^{unc} \in S_1 &\iff i^{c1} \notin c_2, \quad i^{c2} \in c_1, \\
 i^{unc} \in S_2 &\iff i^{c1} \in c_2, \quad i^{c2} \notin c_1, \\
 i^{unc} \in S_3 &\iff i^{c1} \notin c_2, \quad i^{c2} \notin c_1, \quad i_{q,t+1}^{unc} > 0, \\
 i^{unc} \in S_4 &\iff i^{c1} \notin c_2, \quad i^{c2} \notin c_1, \quad i_{q,t+1}^{unc} < 0, \\
 i^{unc} \in S_5 &\iff i^{c1} \in c_2, \quad i^{c2} \in c_1.
 \end{aligned} \quad (32)$$

When none of the projections satisfy both constraints (sets S_3 and S_4), the solution is at the intersection of both ellipses, denoted i_{+}^{int} and i_{-}^{int} . The sign of the q component is equal to the sign of the q component of the unconstrained solution. Note that the ellipses can be also disjoint, e.g. when dc-link voltage suddenly drops in field weakening regime. In such a case, constraint c_1 has higher priority and the optimal solution is $i^{opt} = [-I_{max}, 0]$.

Conditions on the right hand side of (32) allow to design a very efficient algorithm presented in Algorithm 1. Summary of the overall design procedure for the proposed controller is described in Algorithm 2.

IV. SIMULATIONS

The proposed control approach was tested on a system (surface mounted PMSM drive prototype) with parameters

$$\begin{aligned}
 R_s &= 0.28\Omega, & \Psi_{PM} &= 0.2\text{Wb}, \\
 L_{sd} &= 3.5\text{mH}, & L_{sq} &= 4\text{mH},
 \end{aligned} \quad (33)$$

Algorithm 2 Summary of the proposed controller

Off-line: (in PC or higher level computer)

Input: Drive parameters and controller tuning

- 1: Design grid $x^{\text{op}(i)}$, $i = 1, \dots, N$ to cover operating range of the drive
- 2: **for** $i = 1$ **to** N **do**
- 3: Compute linear system matrices (7)
- 4: Solve Riccati equation (14) to obtain $L^{\text{op}(i)}$, $Y^{\text{op}(i)}$.
- 5: Compute the Kalman gain $K^{\text{op}(i)}$
- 6: **end for**
- 7: Solve least squares problem (18) for the controller and observer.

Output: Send coefficients $\alpha_{i,j}$, ζ , K , ϕ to DSP.

On-line: (in DSP)

- 8: Collect measurements
- 9: Compute state estimate \hat{x}_t using (19)
- 10: Evaluate unconstrained control law u_t^{unc} , (35) and (36)
- 11: Compute i^{opt} using (26) and $\bar{i}^{\text{unc}} = \Phi^{\frac{1}{2}} i^{\text{unc}}$
- 12: Update $I_{FW} = \zeta U_{dc} / (\sqrt{3} |\omega| L_d)$
- 13: Run Algorithm 1 to obtain constrained solution \bar{i}^{opt}
- 14: Compute constrained voltage vector u_t using (29)

Output: u_t as the reference for the PWM

sampling time $\Delta t = 125\mu\text{s}$, and dc-link voltage $U_{dc} = 100\text{V}$.

A. SDRE controller

The penalization matrices of the quadratic cost (13) were chosen to be

$$\begin{aligned} Q^{\frac{1}{2}} &= \text{diag}([0.7, 0.7, 1, 0, 0]), \\ R^{\frac{1}{2}} &= 2e-4 \text{diag}([1, 1]). \end{aligned} \quad (34)$$

where notation $2e-4$ is used as abbreviation of 2×10^{-4} . Note that only two parameters were chosen since penalization of the rotor speed can be set to one. The parameters have the following meaning which is useful for their selection:

- 1) The first parameter ($q_{11} = q_{22}$) is equivalent to the parameter λ of the trade off between the speed tracking and current amplitude (11). The lower value of this parameter yields faster settling time of the speed at the cost of lower drive efficiency.
- 2) The second parameter (multiplier of the identity matrix in R) governs the trade off between control performance and control effort. For lower values of the this parameter, the controller has higher gain yielding more aggressive control actions.

Both of these parameters are tuned manually, however, good performance is obtained for a wide range of possible values.

Using (34) and model (7) in the SDRE design procedure with polynomial interpolation, we obtain controller in form

(17)

$$\begin{aligned} u_{d,t}^{\text{unc}} &= -27i_{d,t} - (1.9e-3\omega_t + 1.8e-3i_{q,t})i_{q,t} \\ &\quad - (-6.5e-3\omega_t - 0.2i_{q,t})\Delta\omega + 2e-4i_{d,t}i_{q,t} \\ &\quad - (1.7e-3\omega_t + 0.064i_q)T_{L,t} + 3e-4u_{d,t-1}. \end{aligned} \quad (35)$$

$$\begin{aligned} u_{q,t}^{\text{unc}} &= -32i_{q,t} + 1.7e-3\omega_t - 8.5e-2i_{q,t}i_{d,t} + \\ &\quad - (79 + 3.9e-3i_{d,t} - 2.9e-4i_{q,t}^2)\Delta\omega_t + \\ &\quad + (27 + 7.2e-2i_{d,t} + 2e-4i_{d,t}^2 - 2e-4i_{q,t}^2)T_{L,t} + \\ &\quad - 2.3e-4i_{d,t}^2i_{q,t} + 2.4e-2\delta + 2.5e-4u_{q,t-1}, \end{aligned} \quad (36)$$

where the only requested value is ω^* entering the equation via $\Delta\omega = (\omega_t^* - \omega_t)$. Better results are obtained if $|\Delta\omega|$ is saturated at ω_{max} , which was in our case $\Delta\omega_{\text{max}} = 15$ for all methods.

The second output of the Riccati equation is matrix $Y = \begin{bmatrix} 1.16 & 0.01 \\ 0.01 & 0.96 \end{bmatrix}$ with state-dependent variations lower than 1% of the values which will be neglected. Due to low values of off-diagonal elements, the approximation of the matrix Φ proposed in Section III-B is well justified with $\phi^2 = 1.05$.

B. Comparison with other methods

In the first test, we compare the methods with respect to Joule losses. This correspond to operation on MTPA in the steady state. In the transients, the MTPA is not sufficient condition since it does not consider tracking error. Since no analytical solution is available, we consider numerical solution of optimization problem (8) with cost (11) on receding horizon of length $h = 25$ as a suboptimal indicator where the optimal trajectory lie. We compare the proposed solution with the cascade control presented in [12]. The numerical solution optimizes the same cost as our method and can be used as indicator of the quality of approximation. The cascade control of [12] is tuned to match the chosen cost function as close as possible. We have chosen PI controller

$$T_L^* = k_P \Delta\omega + k_I \Sigma_\omega, \quad (37)$$

where the integrator $\Sigma_\omega = \Sigma_\omega + \Delta\omega$ saturated when its amplitude increases a constant Σ_{max} . Constants of the PI controller are tuned to match the behavior of the SDRE, in this case $k_P = 10$, $k_I = 0.5$, $\Sigma_{\text{max}} = 4$.

Comparison of the tested method was first performed in simulation with perfect state information. For better visibility of the graphs, we show all results in Figure 2 for $I_{\text{max}} = 40A$. Since methods were tuned for similarity, the differences in speed and current response of for all methods at the step change from zero to 40 rad/s are negligible. The only difference is notable at the d - q current plane where deviations from MTPA are studied. We distinguish three phases of the transient: i) current rising edge, ii) operation on current limit, and iii) current falling edge when approaching the speed setpoint. In the rising edge, all algorithms deviate from the MTPA trajectory. The numerical and the proposed algorithm are based on linearization of the system (7) and thus the current follows a tangent to MTPA at each operating point. The controller [12] is heading towards the intersection of the MTPA and the current limit, however due to voltage constraint

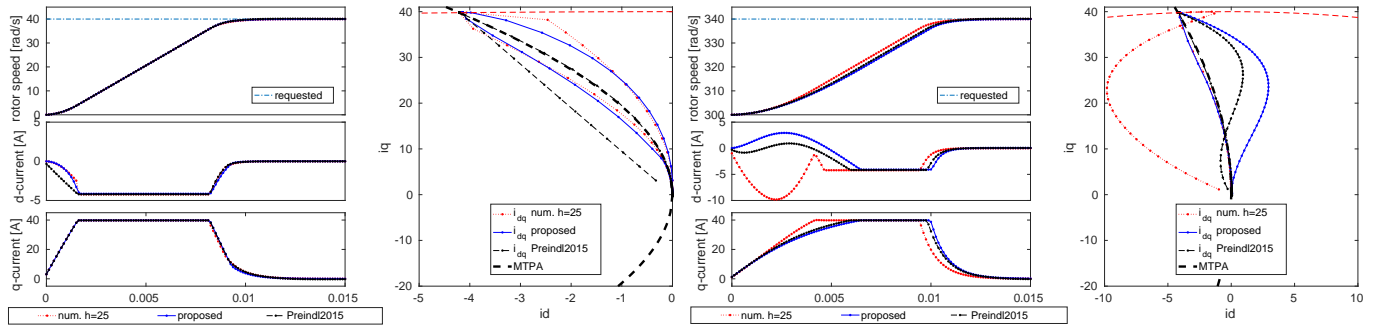


Figure 2. Simulation of step-change of the requested electrical rotor speed from zero to 40 rad/s (left) and from 300 to 340 rad/s (right) under perfect state information. Responses of three compared methods are displayed: numerical solution of optimization problem (8) on horizon $h = 25$, method of [12] and the proposed method. Left part of each profile contains from the top: the time profiles of the rotor speed, d -current and q -current, respectively. Right part represents the i_d, i_q current plane.

it can make only a small step and it is doing it using the shortest trajectory in the Euclidean distance in one step-ahead optimization. In the current limit phase, current trajectories of all algorithms are at the intersection of the MTPA curve and the current limit. In the falling edge, the algorithm [12] follows exactly the MTPA trajectory, while the other two algorithms yield current trajectories slightly below it.

The current rising edge is however very different when the transient happens at higher speed, such as 300 rad/s, Figure 2 right. Algorithm of [12] heads for the intersection point but one step ahead optimization does not result in the shortest trajectory. A similar trajectory, shifted by the linearization error is followed by the proposed solution. The numerical solution has much longer prediction horizon and thus follows a completely different trajectory. Since it searches for a compromise between Joule losses and tracking performance, it sacrifices Joule losses at the beginning to gain lower tracking error later. Specifically, it follows the time-optimal current trajectory (in which the d current is a function of $-\sin(\omega t)$, [20]) to reach the maximum current amplitude as fast as possible. This is best visible in the q -current in Figure 2 right. The resulting torque reaches its maximum sooner yielding faster speed transient than the other methods. The methods of [12] is also marginally faster than the proposed method.

C. Field weakening operation

The results of simulation of the proposed control strategy for a step change of the requested speed from 0 to 230 rad/sec and reversal to -230 rad/sec is displayed in Figure 3. The current vector in dq reference frame follows the MTPA trajectory at the beginning. When the current limit constraint is reached, the trajectory is kept at the intersection of the current limit and MTPA. With increasing speed, the current vector is moved to intersection of the current limit (curve c_1) and FW constraints. As the speed approaches the reference, the torque is decreasing and the current follows the FW curve at the actual speed. As the speed is approaching the requested value, the current is lower than the limit, and follows the FW curve. The current vector leaves c_1 at $\omega = 221$ rad/s and ends at the requested $\omega = 230$ rad/sec, Figure 3. Operation on the intersection of

Table I
EXECUTION TIMES OF STEPS OF THE ALGORITHM

operation	exec. time proposed	exec. time [12]
data acquisition	3.3 μ s	3.3 μ s
Kalman filter	3.1 μ s	3.1 μ s
delay compensation	0.9 μ s	0.9 μ s
SDRE controller	3.0 μ s	
constraint optimization	4.8–6.2 μ s	
PI controller		0.6 μ s
current set-point		9.1–13.3 μ s
CCS current controller	0.8 μ s	0.8 μ s
total	<17.3 μ s	<22.0 μ s

the c_1 and FW constraints is common to the proposed and the method of [12], yielding identical results.

V. EXPERIMENTS

A laboratory prototype of the PMSM drive with the same parameters as in the simulation (33) was used to verify the approach experimentally. The test rig is displayed in Figure 5. The rated power of the PMSM drive is 10.7kW, rated voltage 346V, rated current 30A, and rated speed 3000rpm. However, the loading induction motor drive has maximum torque corresponding to 20A. The PMSM drive is equipped with 12bit absolute angular position encoder LARM ARC 405, torque sensor TW20N, voltage transducer LEM LV 25-P for converter dc-link voltage measurement, and current transducers LA 55-P for measurement of the stator phase currents. The switching frequency of the voltage-source converter supplying PMSM is 8kHz.

The proposed algorithm was implemented in digital signal processor Texas Instruments TMS320F28335. Computational times of individual blocks of the controller are displayed in Table I. The computational time of the constraint optimization varies in the code paths, the worst case scenario is computation of the ellipse intersection (line 9 and 10 of Algorithm 1). Computational time of the method [12] are also displayed in Table I, the most expensive operation is computation of the root of fourth order polynomial for intersection of the torque isoline and MTPA for which we used the Ferrari's method [21]. The numerical optimization was not implemented due to excessive computational requirements.

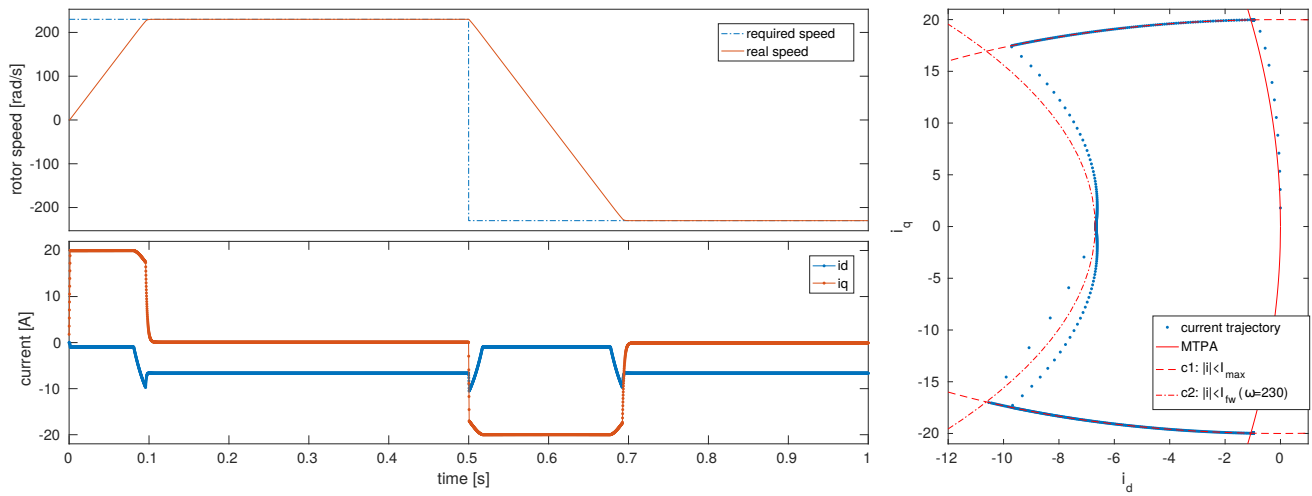


Figure 3. Comparison of the current trajectory of the proposed SDRE controller with the MTPA trajectory and FW constraints on speed control of PMSM drive at startup and speed reversal of electrical rotor speed of $\omega = \pm 230 \text{ rad/s}$ under current limit $I_{max} = 20 \text{ A}$. **Top left:** simulated speed of the drive and speed reference. **Bottom left:** current vector in the dq reference frame. **Right:** trajectory of the current vector in the dq plane and its comparison with the MTPA trajectory and FW constraints.

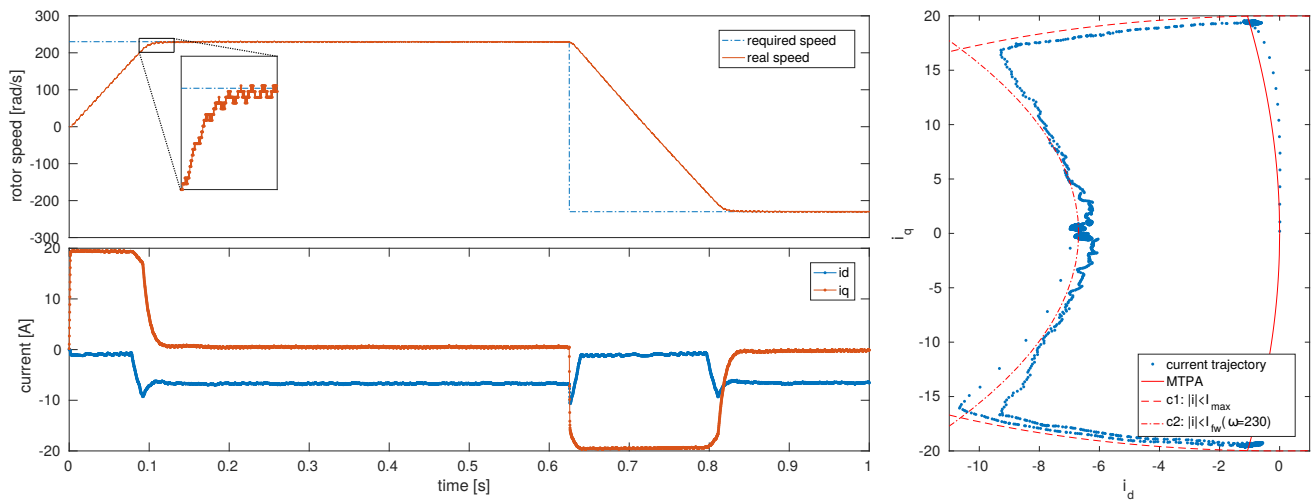


Figure 4. Speed control of PMSM drive at startup and speed reversal of electrical rotor speed of $\omega = \pm 230 \text{ rad/s}$ under current limit $I_{max} = 20 \text{ A}$. **Top left:** measured speed of the drive and speed reference. **Bottom left:** current vector in the dq reference frame. **Right:** trajectory of the current vector in the dq plane and its comparison with the MTPA trajectory and FW constraint.

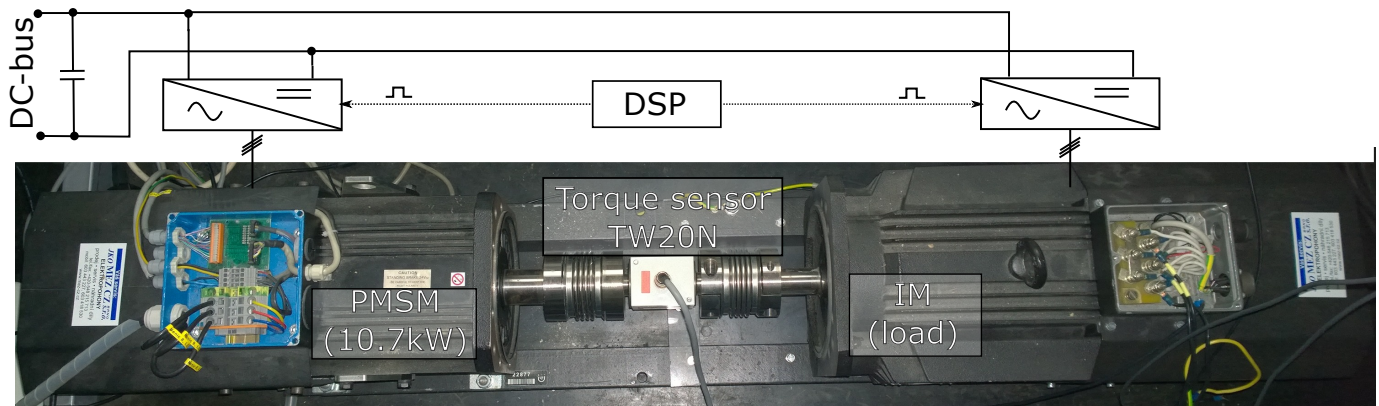


Figure 5. Photo of the experimental test rig with the controlled PMSM and loading induction machine.

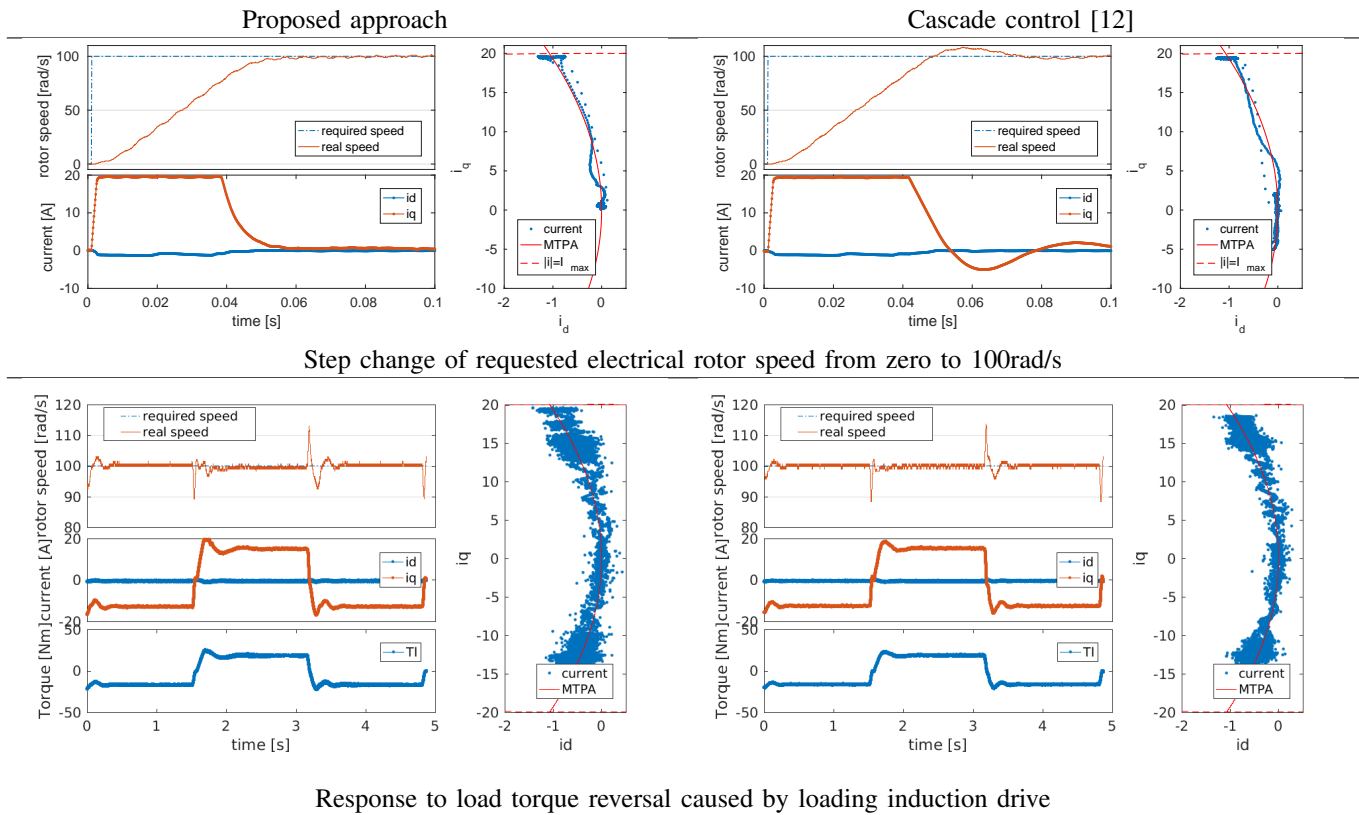


Figure 6. Comparison of the proposed direct speed control (left column) with the cascade method of [12] (right column) on step change of the requested electrical rotor speed (top row) and load reversal operation (bottom row).

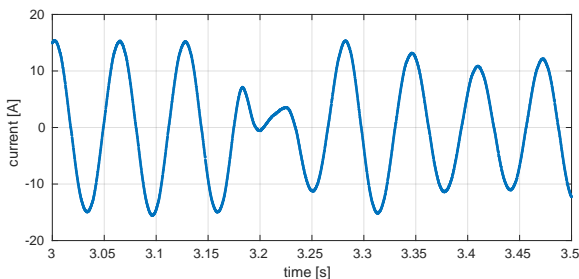


Figure 7. Phase a of the stator current of the proposed control of the PMSM drive during transient of the load from from 18Nm to -16.8 Nm. It corresponds to time index 3–3.5s in Figure 6 bottom row.

The proposed controller was using the same matrix Q as in the simulation but matrix R was changed to $R = 4e-2 \text{diag}([1, 1])$. Since the state of the drive is not perfectly known, it is replaced by output of the Kalman observer which was designed with covariance matrices $\Sigma_x = \text{diag}(1, 1, 1e-4, 0, 0, 1)$ and $\Sigma_y = \text{diag}(1, 1, 0.004)$. The same observer was used for both of the compared methods. However, all state variables in the subsequent figures are displayed before any filtering to visualize real conditions as closely as possible. In the figures, the rotor speed is obtained by numerical differentiation of the rotor position on window of length 70 samples. Therefore, quantization effect of the rotor position encoder are visible as a ripple on the unfiltered speed. Experimental results of the startup and speed reversal of ± 230

rad/s are displayed in Figure 4. Note that the current vector operates within the constraints in the same manner as in simulations. Slight fluctuations of the current are caused by imperfect state information from the observer, cogging and minor fluctuations of the dc-link voltage.

Comparison with the cascade approach of [12] is presented in Fig. 6 in step change of the requested electrical rotor speed, and under torque load reversal profile generated by the loading induction machine. The gains of the PI controller in the cascade control were tuned to match the load response of the proposed approach. Same maximum speed error was achieved for gains $k_P = 1$ and $k_I = 0.02$, but the integration saturation Σ_{\max} had to be increased to 1000 in order to track the load torque. Due to the increased integration saturation limit, the PI controller generates larger overshoots² on the speed at the step change of the requested value, see Figure 6 top row. Since the SDRE controller has richer structure, using both the estimate of the torque, T_L , and its derivative, δ , in the control law (35)–(36), it does not require the integration saturation limit and provides smooth transition under the step change of the required rotor speed.

The corresponding current trajectories in the dq current plane are displayed on the right side next to each profile. Note that in the step change of the required rotor speed, Figure 6 top row, the rising edge of the current corresponds to simulation while falling edge in both cases deviates from the MTPA due

²This particular problem can be solved by feed-forward, which however results in deteriorated performance in steady state.

to imperfect state reconstruction. The deviation is larger for both methods in the load reversal operation, Figure 6 bottom.

VI. CONCLUSION

In this paper, we proposed an algorithm for direct speed control of a PMSM drive. It combines results of unconstrained control strategy and convex optimization that guarantees satisfaction of explicit constraints on the maximum amplitude of the stator current and field weakening operation. The unconstrained solution is used without any modification when the constraints are not active. Activation of the constraints is expected only in rapid transients and field weakening operation. The method uses a precomputed constants for online computation of state dependent weights. Computation of these constants can be done either in the initialization phase of the DSP or in master control unit of DSP. Since it complicates the commissioning, it is worth in applications that require high quality of control. We expect that the proposed algorithm will be advantageous for development of control algorithms for more demanding applications. Many extensions of the state space models including dynamics of the loading torque or spectrum weighted penalizations on the phase currents has been proposed in the literature. For such models, the resulting SDRE would be different, however, the code of the constrained optimization would remain the same. Therefore, the proposed optimization scheme can be easily applied even to other state space based control methods, such as adaptive, fuzzy or neural network controls.

APPENDIX

A. Fast projection of vector to an ellipse

Using parametrization of an ellipse $[a \cos \varphi, b \sin \varphi]$, the distance to a vector $[x_0, y_0]$ is minimal when

$$x_0 a \sin \varphi - y_0 b \cos \varphi = (a^2 - b^2) \sin \varphi \cos \varphi, \quad (38)$$

which is established by setting derivative of the distance to zero. Using substitution $[s = \sin \varphi, c = \cos \varphi]$, solution of (38) is equivalent to solution of

$$\begin{aligned} x_0 a s - y_0 b c - (a^2 - b^2) s c &= 0, \\ s^2 + c^2 - 1 &= 0, \end{aligned} \quad (39)$$

which can be solved by the Newton's method. Specifically, its first iteration is

$$\begin{aligned} s_{k+1} &= s_k - 2\delta c(x_0 a s - y_0 b c - \alpha s c), \\ c_{k+1} &= c_k - 2\delta s(x_0 a s - y_0 b c - \alpha s c), \\ \delta &= (c x_0 a + s y_0 b + \alpha(s^2 - c^2))^{-1}, \\ \alpha &= (a^2 - b^2), \end{aligned}$$

and the subsequent ones are only slightly more complex. The iterations are initialized at point

$$s_0 = \frac{y_0}{\sqrt{x_0^2 + y_0^2}}, \quad c_0 = \frac{x_0}{\sqrt{x_0^2 + y_0^2}}.$$

One iteration of the Newton's algorithm was found sufficiently accurate if a and b are on comparable scale. More iterations

are needed if $a \ll b$ or $a \gg b$. After the final iteration, the solution is projected to guarantee (39) to yield

$$x_{proj} = \frac{a c_k}{\sqrt{c_k^2 + s_k^2}}, \quad y_{proj} = \frac{b s_k}{\sqrt{c_k^2 + s_k^2}}. \quad (40)$$

B. Ellipse intersection

The \bar{i}_d^{int} current of the intersection of ellipses (30) and (31) is a root of polynomial

$$\bar{i}_d^2(1 - \xi) + 2i_d i_d^\psi + (i_d^\psi)^2 - I_{FW}^2 + I_{\max}^2 \xi = 0 \quad (41)$$

and \bar{i}_q^{int} is evaluated from (30) as $\bar{i}_q^{\text{int}} = \pm \sqrt{I_{\max}^2 - (\bar{i}_d^{\text{int}})^2} \phi$.

REFERENCES

- [1] D. Bertsekas, *Dynamic Programming and Optimal Control*. Nashua, US: Athena Scientific, 2001, 2nd edition.
- [2] T.-S. Low, T.-H. Lee, and K.-T. Chang, "An optimal speed controller for permanent-magnet synchronous motor drives," in *Industrial Electronics, Control, Instrumentation, and Automation, 1992. Power Electronics and Motion Control, Proceedings of the 1992 International Conference on*, DOI 10.1109/IECON.1992.254572, pp. 407–412 vol.1, Nov. 1992.
- [3] T. D. Do, H. H. Choi, and J.-W. Jung, "Sdre-based near optimal control system design for pm synchronous motor," *IEEE Transactions on Industrial Electronics*, vol. 59, DOI 10.1109/TIE.2011.2174540, no. 11, pp. 4063–4074, Nov. 2012.
- [4] T. D. Do, S. Kwak, H. H. Choi, and J.-W. Jung, "Suboptimal control scheme design for interior permanent-magnet synchronous motors: An sdre-based approach," *IEEE Transactions on Power Electronics*, vol. 29, DOI 10.1109/TPEL.2013.2272582, no. 6, pp. 3020–3031, Jun. 2014.
- [5] R. Errouissi, M. Ouhrouche, W.-H. Chen, and A. M. Trzynadlowski, "Robust nonlinear predictive controller for permanent-magnet synchronous motors with an optimized cost function," *IEEE Transactions on Industrial Electronics*, vol. 59, no. 7, pp. 2849–2858, 2012.
- [6] T. Tarczewski and L. M. Grzesiak, "Constrained state feedback speed control of pmsm based on model predictive approach," *IEEE Transactions on Industrial Electronics*, vol. 63, DOI 10.1109/TIE.2015.2497302, no. 6, pp. 3867–3875, Jun. 2016.
- [7] J. Rodríguez, M. Kazmierkowski, J. Espinoza, P. Zanchetta, H. Abu-Rub, H. Young, and C. Rojas, "State of the art of finite control set model predictive control in power electronics," *IEEE Transactions on Industrial Informatics*, vol. 9, DOI 10.1109/TII.2012.2221469, no. 2, pp. 1003–1016, 2013.
- [8] M. Preindl and S. Bolognani, "Model predictive direct torque control with finite control set for pmsm drive systems, part 1: Maximum torque per ampere operation," *IEEE Transactions on Industrial Informatics*, vol. 9, DOI 10.1109/TII.2012.2227265, no. 4, pp. 1912–1921, Nov. 2013.
- [9] M. Preindl and S. Bolognani, "Model predictive direct torque control with finite control set for pmsm drive systems, part 2: field weakening operation," *IEEE Transactions on Industrial Informatics*, vol. 9, no. 2, pp. 648–657, 2013.
- [10] E. Fuentes, D. Kalise, J. Rodríguez, and R. Kennel, "Cascade-free predictive speed control for electrical drives," *IEEE Transactions on Industrial Electronics*, vol. 61, DOI 10.1109/TIE.2013.2272280, no. 5, pp. 2176–2184, May. 2014.
- [11] M. Preindl and S. Bolognani, "Model predictive direct speed control with finite control set of pmsm drive systems," *IEEE Trans. Power Electron.*, vol. 28, no. 2, pp. 1007–1015, 2013.
- [12] M. Preindl and S. Bolognani, "Optimal state reference computation with constrained mtpa criterion for pm motor drives," *IEEE Transactions on Power Electronics*, vol. 30, no. 8, pp. 4524–4535, 2015.
- [13] M. Preindl, "Robust control invariant sets and lyapunov-based mpc for ipm synchronous motor drives," *IEEE Transactions on Industrial Electronics*, vol. 63, DOI 10.1109/TIE.2016.2527722, no. 6, pp. 3925–3933, Jun. 2016.
- [14] D. Limón, I. Alvarado, T. Alamo, and E. F. Camacho, "Mpc for tracking piecewise constant references for constrained linear systems," *Automatica*, vol. 44, no. 9, pp. 2382–2387, 2008.
- [15] J. Lemmens, P. Vanassche, and J. Driesen, "Pmsm drive current and voltage limiting as a constraint optimal control problem," *IEEE Transactions on Industrial Electronics*, 2014.

- [16] A. Damiano, G. Gatto, I. Marongiu, A. Perfetto, and A. Serpi, "Operating constraints management of a surface-mounted pm synchronous machine by means of an fpga-based model predictive control algorithm," *IEEE Transactions on Industrial Informatics*, vol. 10, DOI 10.1109/TII.2013.2261304, no. 1, pp. 243–255, Feb. 2014.
- [17] V. Šmídl, V. Mácha, Š. Janouš, and Z. Peroutka, "Analysis of cost functions and setpoints for predictive speed control of pmsm drives," in *Power Electronics and Applications (EPE), 2016 18th European Conference on*, pp. 1–6. IEEE, 2016.
- [18] H. Banks, B. Lewis, and H. Tran, "Nonlinear feedback controllers and compensators: a state-dependent riccati equation approach," *Computational Optimization and Applications*, vol. 37, no. 2, pp. 177–218, 2007.
- [19] R. Kalman, "A new approach to linear filtering and prediction problem," *Trans. ASME, Ser. D, J. Basic Eng.*, vol. 82, pp. 34–45, 1960.
- [20] N. Bianchi, S. Bolognani, and M. Zigliotto, "Time optimal current control for pmsm drives," in *IECON 02 [Industrial Electronics Society, IEEE 2002 28th Annual Conference of the]*, vol. 1, pp. 745–750. IEEE, 2002.
- [21] S.-Y. Jung, J. Hong, and K. Nam, "Current minimizing torque control of the ipmsm using ferrari's method," *IEEE Transactions on Power Electronics*, vol. 28, no. 12, pp. 5603–5617, 2013.



Václav Šmídl (M'05) received Ph.D. degree in Electrical Engineering from Trinity College Dublin, Ireland in 2004. Since 2004, he is a researcher in the Institute of Information Theory and Automation, Prague, Czech Republic. In October 2010 he joined the Regional Innovation Centre for Electrical Engineering, RICE. His research interests are advanced estimation and control techniques and their applications. He published one research monograph, twenty journal papers and over 90 conference papers.



Štěpán Janouš received master degree in Electrical Engineering from the University of West Bohemia (UWB), Pilsen, Czech Republic in 2011, where he is currently working on his Ph.D. degree. In 2013 he joined the Regional Innovation Centre for Electrical Engineering, RICE. His research interests are advanced control techniques for drives and power converters.



Lukáš Adam received his Ph.D. degree in 2015 at the Charles University in Prague, Czech Republic. At 2012 he started working at the Institute of Information Theory and Automation, Prague, Czech Republic and in 2015 he moved to the Humboldt University of Berlin, Germany. Initially working in nonsmooth optimization, he later became interested in optimization with PDE constraints. He tries to apply his theoretical knowledge by cooperating with engineers. He is an author of more than ten journal papers.



Zdeněk Peroutka (S'01–M'04) received master and PhD degrees in Electrical Engineering from the University of West Bohemia (UWB), Pilsen, Czech Republic in 2000 and 2004, respectively. He is Full Professor of Power Electronics and Control Systems and Vice-Dean for Science and Strategy at the Faculty of Electrical Engineering at UWB. From 2010 to 2016, he was a Scientific Director and Principal Investigator of the Regional Innovation Centre for Electrical Engineering (RICE) at UWB. Since 2016, he is

a CEO and Principal Investigator of RICE. His main research topic is control of drives of modern transport systems and vehicles, and power electronics converters for medium-voltage applications. He published more than 150 papers in international journals and conferences. He is inventor of two international patents..